



This is a repository copy of *The application of artificial intelligence to microarray data: identification of a novel gene signature to identify bladder cancer progression.*

White Rose Research Online URL for this paper:
<http://eprints.whiterose.ac.uk/10439/>

Article:

Catto, J.W.F., Abbod, M.F., Wild, P.J. et al. (10 more authors) (2010) The application of artificial intelligence to microarray data: identification of a novel gene signature to identify bladder cancer progression. *European Urology*, 57 (3). pp. 398-406. ISSN 0302-2838

<https://doi.org/10.1016/j.eururo.2009.10.029>

Reuse

Unless indicated otherwise, fulltext items are protected by copyright with all rights reserved. The copyright exception in section 29 of the Copyright, Designs and Patents Act 1988 allows the making of a single copy solely for the purpose of non-commercial research or private study within the limits of fair dealing. The publisher or other rights-holder may allow further reproduction and re-use of this version - refer to the White Rose Research Online record for this item. Where records identify the publisher as the copyright holder, users can verify any specific terms of use on the publisher's website.

Takedown

If you consider content in White Rose Research Online to be in breach of UK law, please notify us by emailing eprints@whiterose.ac.uk including the URL of the record and the reason for the withdrawal request.



eprints@whiterose.ac.uk
<https://eprints.whiterose.ac.uk/>

promoting access to White Rose research papers



Universities of Leeds, Sheffield and York
<http://eprints.whiterose.ac.uk/>

This is an author produced version of a paper published in **European Urology**.

White Rose Research Online URL for this paper:

<http://eprints.whiterose.ac.uk/10439>

Published paper

Catto, J.W.F., Abbod, M.F., Wild, P.J., Linkens, D.A., Pilarsky, C., Rehman, I., Rosario, D.J., Denzinger, S., Burger, M., Stoehr, R., Knuechel, R., Hartmann, A., Hamdy, F.C., *The application of artificial intelligence to microarray data: identification of a novel gene signature to identify bladder cancer progression*, *European Urology*, 57 (3), pp. 398-406

<http://dx.doi.org/10.1016/j.eururo.2009.10.029>

The application of artificial intelligence to microarray data: Identification of a novel gene signature to identify bladder cancer progression

James W.F. Catto PhD^{1§*}, Maysam F. Abbod PhD^{2§}, Peter J. Wild MD^{3§}, Derek A. Linkens PhD⁴, Christian Pilarsky PhD⁵, Ishtiaq Rehman PhD¹, Derek J. Rosario MD¹, Stefan Denzinger MD⁶, Maximilian Burger MD⁶, Robert Stoehr PhD⁷, Ruth Knuechel MD⁸, Arndt Hartmann MD^{7#} and Freddie C. Hamdy MD^{9#}

¹Academic Urology Unit and ⁴ Department of Automatic Control and Systems Engineering, University of Sheffield, UK; ² School of Engineering and Design, Brunel University, West London, UB8 3PH; ³ Institute for Surgical Pathology, University Hospital Zurich, Switzerland; ⁵ Department of Surgery, University of Dresden, Germany; ⁶ Department of Urology, University of Regensburg, Germany, ⁷ Department for Pathology, University of Erlangen, Germany; ⁸ Institute of Pathology, University of Aachen, Germany; ⁹ Nuffield Department of Surgery, University of Oxford, Oxford, UK;

[§]These authors contributed equally to this work

[#] These authors share senior authorship of this work

*Address for correspondence; James Catto, Academic Urology Unit, K Floor, Royal Hallamshire Hospital, Glossop road, SHEFFIELD, S10 2JF, United Kingdom, Tel: +44 +114 271 2154. Fax: +44 +114 271 2268 Email: J.Catto@sheffield.ac.uk

Running title: Microarray interrogation using artificial intelligence

MESH words: Artificial Intelligence, Gene array, Bladder Cancer, Prognosis

Word count:

Text = 2344

Figures = 4 and Tables = 2

References = 30

Abstract word count: 257

Abstract

Background: New methods to identify bladder cancer progression are required. Gene-expression microarrays can reveal insights into disease biology and identify novel biomarkers. However, these experiments produce large datasets that are hard to interpret.

Objective: To develop a novel method of microarray analysis combining two forms of artificial intelligence (AI): NeuroFuzzy Modeling (NFM) and Artificial Neural Networks (ANN). To validate this in a bladder cancer cohort.

Design, Setting, and Participants: We used AI and statistical analyses to identify progression-related genes in a microarray dataset (n=66 tumors, n=2,800 genes). The AI-selected genes were then investigated in a second cohort (n=262 tumors) using immunohistochemistry.

Measurements: We compared the accuracy of AI and statistical approaches to identify tumor progression.

Results and limitations: AI identified 11 progression-associated genes (OR=0.70 (95% CI=0.56-0.87) p=0.0004) and these were more discriminate than genes chosen using statistical analyses (OR=1.24 (95% CI=0.96-1.60) p=0.09). The expression of 6 AI-selected genes (LIG3, Fas, KRT18, ICAM1, DSG2 and BRCA2) was determined using commercial antibodies and successfully identified tumor progression (Concordance

Index=0.66, Logrank $p=0.01$). AI-selected genes were more discriminate than pathological criteria at determining progression (Cox multivariate analysis $p=0.01$). Limitations include the use of statistical correlation to identify 200 genes for AI analysis and that we did not compare regression identified genes with immunohistochemistry.

Conclusions: AI and statistical analyses use different techniques of inference to determine gene-phenotype associations and identify distinct prognostic gene signatures that are equally valid. We have identified a prognostic gene signature, whose members reflect a variety of carcinogenic pathways, which could identify progression in non-muscle invasive bladder cancers.

Introduction

The care of patients with Urothelial Carcinoma of the bladder (UCC) could be significantly improved if their tumor behavior was accurately identified at diagnosis. Patients with non-progressive superficial disease could be spared endoscopic surveillance and BCG immunotherapy, whilst those at high progression risk could opt for early cystectomy. For invasive tumors the use of systemic chemotherapy could be rationalized to cases with highest progression risk. Tumor behavior can be hard to determine from histopathology alone. For example, the progression risk for non-muscle UCC varies between <1% and >50% [1, 2]. Furthermore, as stage and grade are often linked, when one is fixed (e.g. stage) the other performs poorly (e.g. grade) at identifying tumor progression. It is hoped that molecular knowledge will reveal an understanding of tumor biology that allows accurate phenotype identification.

As current biomarkers are insufficiently robust for clinical practice, microarrays have been used to identify new candidates [3] [4]. Microarray experiments reveal great insights into tumor biology but the cost and magnitude of these experiments prohibit large sample size analyses. Thus, microarray datasets have high dimensionality (large imbalance between gene number and sample size) that leads to analytical difficulties [5] [6] [7]. Successful analysis requires the identification of genes related to tumor-class and the removal of non-contributing variables. Poor analysis leads to data over-fitting and irreproducible results [5]. Traditional analytical techniques, such as hierarchical clustering, assume biological linearity and use statistical proximity to infer class-gene relationships (so called ‘feature selection’). They perform poorly in datasets

contaminated with variable noise. Artificial intelligence (AI) is a machine learning approach without these prerequisites. Various AI techniques exist [8] and successful microarray analysis has been reported using artificial neural networks (ANN) [9] [10] and support vector machines (SVMs) [11, 12] in non-urothelial malignancies. However, the hidden working layer of an ANN prevents model understanding and hinders its acceptance by the scientific community [13], whilst SVMs still use proximity to infer class-gene associations and function poorly with respect to interpretability [14].

An alternative form of AI is the neurofuzzy model (NFM). This has a similar design to an ANN, but uses a transparent fuzzy logic internal structure [8]. This transparency allows model understanding, parameter interrogation and can facilitate the inclusion of priori qualitative knowledge. When used to identify tumor progression we have previously found that NFM is accurate, reproducible and appears superior to regression based classifications [15, 16]. We hypothesized that NFM could improve microarray analysis and identify prognostic gene panels that could accurately predict the behavior of UCC. To test this hypothesis we examined a previously reported non-muscle invasive UCC microarray dataset to find genes associated with progression to invasion. Genes associated with progression were then tested in a new larger UCC cohort using immunohistochemistry.

Materials and methods

Patients and Tumors

We studied two patient populations (Table 1). For microarray analysis we used 66 tumors from 34 patients, treated at the Ludwig Maximilian University, Germany (detailed in [17]). Progression to muscle invasion occurred in 10/34 patients (29%) and the median follow up was 43 months. For immunohistochemical analysis we studied 262 tumors from separate consecutive patients treated at the University of Regensburg, Germany. We created a tissue microarray (TMA) using paraffin embedded formalin fixed tissues with 2 cores per cases (1.2mm) [18]. Progression information was available for 182/262 (69.5%) patients and muscle invasion or new metastases occurred in 49 patients (26.9%). The median follow up was 89 months (range 2-154). No patients were in both UCC populations. Normal urothelium from patients with benign prostatic hyperplasia (n=20) and co-existing UCC (n=15) was also analyzed. Institutional review board approval was obtained from both institutions prior to study commencement.

RNA Extraction and Gene Expression Microarray Analysis

The microarray (metg001A) contained 2,800 genes (6,117 probesets) annotated by the GoldenPath assembly. The microarray experiments and data processing are reported in detail elsewhere [17].

Artificial Intelligence Feature Selection

To analyze the microarray data we used a ‘Committee of models’ approach that assimilated findings from each individual AI model (Figure 1), as we wanted to

determine gene-progression relationships that were not dependent upon one AI structure. We initially performed a dimension reduction using Pearson's coefficient to identify the 200 genes most associated with progression. These selected genes were then analyzed using iterative ANN and NFM models in two structures, which we termed '*Selectivity*' and '*Averaging*' (Figure 1). These structures enable simultaneous analysis of all genes, rather than a '*Leave-One-Out*' approach. ANNs were produced within Statistica (Version 7, StatSoft Ltd, Bedford, UK). NFMs were produced within Matlab (Version 6.5 www.mathworks.com) and progression predictions performed using an in-house software suite [19, 20]. The data were divided into 90% for training (60% was learning and 30% for validation) and 10% for testing. Ensembling and cross validation were used to maximize data [21].

We ranked the 200 genes according to the size of model error induced by their alteration. Those with largest error were ranked highest, as alteration of their values produced the largest disturbance in the models accuracy. For each gene a '*Committee*' ranking was produced from the average score of the individual AI models. A panel of progression related genes was produced from those with the highest ranking. This *Committee* panel was compared with the '*Original*' gene panel selected using Pearson's linear regression coefficient and GeneCluster 2.0 software [17]. This *Original* panel included 11 members (FABP4, GSTM4, SERPINA1, HDAC1, C20ORF1, DNLC2A, PTK6 UBC, MGMT, ITGB3BP and PAIP2).

Immunohistochemistry

To evaluate the *Committee* approach we analyzed the expression of its highest ranking members using immunohistochemistry in a new UCC cohort [17, 22]. Commercially manufactured antibodies were available for six members: LIG3 (clone 6G9; Abcam, Cambridge, UK; dilution 1:50), BRCA2 (Abcam, Cambridge, UK; dilution 1:10), TNFRSF6 (Abcam, Cambridge, UK; dilution 1:25), KRT18 (clone CK2; Chemicon, Billerica, MA, USA; dilution 1:50), DSG2 (clone 3G132; Abcam, Cambridge, UK; dilution 1:10), and ICAM1 (clone 23G12; Lab Vision, Fremont, CA, USA; dilution 1:10). For negative controls the primary antibody was omitted. Immunostained sections were scored independently for the percentage of positive tumor cells by uropathologists (PW, AH). The abnormal status for each protein was defined according to its cellular function, its contrast with normal urothelial expression and from previous reports. For ICAM1, a case was considered positive if > 30% of intra-tumoral blood vessels were stained. For LIG3, BRCA2, TNFRSF6, and DSG2 abnormal expression was defined as a loss or reduction of staining (0% or $\leq 30\%$ positively stained cells). For both, normal urothelium had expression in >50% of cells. Abnormal KRT18 expression was defined as increased immunostaining ($\geq 80\%$ cells with positive staining) with respect to normal samples, which were negative in 90% of cases.

Statistical Analysis

All analyses were two tailed and carried out using SPSS (version 14, SPSS Inc). Categorical variables were compared using the χ^2 test and continuous variables with a T test. Disease progression was defined when a non-muscle invasive tumor became invasive or a muscle invasive tumor developed metastases. Progression-specific survival

probability following tumor resection was analyzed using the Kaplan-Meier method and Log rank test. Patients without progression were censored when they were last reviewed or when they died of other causes. The concordance index was calculated as reported [23]. A P value of <0.05 was interpreted as statistically significant. Cox regression multivariate analysis was used to compare the prognostic value of the various gene panels with clinicopathological parameters.

Results

Dimension reduction

We aimed to produce a prognostic gene panel of around 11 members to allow comparison with the *Original* panel chosen by statistical methods. Analysis of predictive ANN and NFM models with increments of 1 to 200 members revealed this was feasible (Figure 2). For NFM, the modeling error with 11 genes (RMS=0.135) was similar to that for more than 157 genes (both concordance index=1.0). For ANN the error did not change until more than 140 gene inputs were used (RMS = 0.37 for 11 genes), and was larger than the equivalent for NFM.

Gene Ranking and Comparison of Feature Selection Panels

We ranked the 200 genes according to their average score from the various AI models (Table 2) and selected the 11 highest ranked genes to compare with the *Original* panel. Using gene expression, dichotomized around the mean, both panels were able to stratify tumor progression, although the *Committee* panel appeared more discriminate. For example, the findings of the *Committee* panel are typical (Figure 3a): whilst individual members are associated with tumor progression (e.g. LIG3 p=0.01, KRT18 p=0.04, Log rank values), the best prediction of progression occurs when the members are used in combination ($\geq 3/11$ abnormal genes p=0.007, $\geq 4/11$ p=0.0004, $\geq 5/11$ p=0.002, Log rank values). In multivariate analysis the *Committee* panel (OR=0.70 (95% CI 0.56-0.87), Logrank p=0.0004) was better at identifying progression than grade (OR=0.38 (95% CI 0.15-0.91, p=0.001) and stage (OR=0.65 (95% CI 0.1-4.31), p=0.03), and the *Original*

panel (OR=1.24 (95% CI 0.96-1.60), p=0.09). No members were shared between the *Committee* and *Original* panels.

Analysis of the Committee panel in a second tumor cohort

Six of the 11 members in the *Committee* panel (LIG3, BRCA2, TNFRSF6, KRT18, DSG2 and ICAM1, Figure 4a) have commercially manufactured antibodies with proven reproducible staining patterns in formalin fixed paraffin embedded tissue. Using these antibodies we performed immunohistochemistry on the 262 tumor TMA. When protein expression was analyzed with respect to tumor histology, various associations were seen. For example, LIG3 and ICAM1 were associated with tumor stage and grade (χ^2 p<0.05) (Table 3), when compared to tumors with normal expression. However, when expression of individual proteins with respect to tumor behavior was analyzed, few significant relationships were present. Only abnormal TNFRSF6 expression was significantly associated with tumor progression (Log rank p=0.003).

We then analyzed the 6 proteins together as a *Committee* panel using only superficial tumors (n=134). Each tumor was scored according to the number of proteins with abnormal staining and this was expressed as a percentage of the total number successfully immunostained for that sample. Only samples with ≥ 4 stained proteins were evaluated. When progression was analyzed with respect to this score, significantly worse outcomes were present in tumors with higher than lower scores (Figure 4b). As with its use in the first tumor cohort, the panel's discriminating ability was maximal at its mean content (Concordance index =0.66, Log rank p=0.02 for 40% and p=0.01 for 50%). In

multivariate analysis, the *Committee* panel was better at stratifying progression (Cox OR=1.2 (95% CI 1.1-1.3), p=0.014) than tumor stage (OR=1.44 (95% CI 0.82-2.53), p=0.2), grade (OR=0.93 (95% CI 0.53-1.66), p=0.8), the presence of CIS (OR=1.3 (95% CI 0.54-3.12), p=0.6), growth pattern (OR=0.74 (95% CI 0.26-2.12), p=0.6) and multifocality (OR=1.61 (95% CI 0.61-4.24), p=0.3).

Discussion

Here we have used AI to examine the relationship between gene expression and progression. To evaluate this approach, rather than specific model designs, we used a Committee of models to merge gene rankings from individual models and structures. AI can identify complex relationships within non-linear data contaminated by variable noise and as such, can outperform statistical regression [8, 24]. AI modeling is a generic process and these methods could be applied to re-interrogate microarray datasets for prognostic and functional data.

Our approach reduced 200 genes to 11 with minimal deterioration in progression identification. The highest ranked genes appeared better at predicting tumor outcome than those selected using traditional analysis and pathological criteria. The fuzzy logic layer of our *Committee* NFM is shown in Figure 3b. This rule-base consists of parallel rules in which the fuzzy logic component can be visualized. In rule 1 (top line), high KRT18 in combination with low DSG2 and TNFRSF6 expression leads to rapid tumor progression (final box). This supports known carcinogenic functions of these genes as KRT18 is an oncogene and the others are tumor suppressors [25]. One can also see that the discriminatory effects in TP53BP2 are less apparent than for other genes (TP53BP2 was ranked 11th, Table 2).

The ability of AI to determine non-linear relationships is demonstrated in our results. Of the 11 genes that comprise the *Committee* panel, only TNFRSF6 was individually associated with tumor progression. However, the cumulative use of this panel allowed

accurate progression discrimination (Figure 4b). The members of the *Committee* panel represent various carcinogenic pathways. Their association with progression may be directly through carcinogenic roles or as bystanders associated with progression. Their diversity in roles suggests they may function as synergistic facilitators of progression. Apoptosis evasion is represented by reduced expression of Fas (TNFRSF6), TP53BP2 and ARHE. Fas is important for apoptosis induction and decreased expression is associated with advanced bladder cancer stage, grade and progression [26]. TP53BP2 (also ‘Apoptosis stimulating protein of p53 2’ (ASPP2)) plays a key role in apoptosis induction through the activation of p53. Reduced TP53BP2 expression abrogates the onset of apoptosis in cancer, but has not been reported in UCC. Tumor invasion is represented by reduced cellular adhesion (ICAM1 and DSG2) and cytoskeletal reorganization through increased KRT18 and reduced ARHE expression. DSG2 is a cellular adhesion molecule whose loss reduces adhesion, increases invasion and speeds tumor progression [27]. ICAM1 is also an intercellular adhesion molecule and is frequently epigenetically silenced in UCC (>70%) [28]. KRT18 is a cytokeratin known to be expressed in the umbrella layer of urothelium whose expression increases with urothelial carcinogenesis [25]. ARHE (also ‘Rho family GTPase 3’ (RND3)) is a Rho signal transduction member with roles in many cellular processes (cytoskeleton organization, membrane trafficking, cell growth and apoptosis) [29], whose loss is reported in prostate cancer. Deranged DNA repair is represented by BRCA2 and LIG3 [30]. Whilst neither is directly linked with bladder carcinogenesis, it is possible that loss of both is required for carcinogenic alteration. BRCA2-deficient cells have reduced DNA ligation capacity which can be reversed by LIG3 administration [30].

Conclusion

AI can analyze microarray datasets in a complementary manner to statistical analyses. Both methods use different techniques of inference to determine gene-phenotype associations and thus identify distinct prognostic gene signatures that are equally valid. We have identified a new prognostic gene signature in UCC, whose members reflect a variety of carcinogenic pathways. This signature requires validation in new tumor cohorts to assess its ability to identify progression in non-muscle invasive bladder cancers.

Conflict of interest

We declare no conflicts of interest with this work.

REFERENCES

1. van Rhijn BW, Burger M, Lotan Y, Solsona E, Stief CG, Sylvester RJ, et al. Recurrence and Progression of Disease in Non-Muscle-Invasive Bladder Cancer: From Epidemiology to Treatment Strategy. *Eur Urol*. 2009. Jun 26 [Epub]
2. Sylvester RJ, van der Meijden AP, Oosterlinck W, Witjes JA, Bouffieux C, Denis L, et al. Predicting recurrence and progression in individual patients with stage Ta T1 bladder cancer using EORTC risk tables: a combined analysis of 2596 patients from seven EORTC trials. *Eur Urol*. 2006;49:466-5
3. Dyrskjot L, Thykjaer T, Kruhoffer M, Jensen JL, Marcussen N, Hamilton-Dutoit S, et al. Identifying distinct classes of bladder carcinoma using microarrays. *Nat Genet*. 2003;33:90-6.
4. Dyrskjot L, Zieger K, Real FX, Malats N, Carrato A, Hurst C, et al. Gene expression signatures predict outcome in non-muscle-invasive bladder carcinoma: a multicenter validation study. *Clin Cancer Res*. 2007;13:3545-51.
5. Ransohoff DF. Rules of evidence for cancer molecular-marker discovery and validation. *Nat Rev Cancer*. 2004;4:309-14.
6. Hamdy FC, Catto JW. Less is more: artificial intelligence and gene-expression arrays. *Lancet*. 2004;364:2003-4.
7. Dupuy A, Simon RM. Critical review of published microarray studies for cancer outcome and guidelines on statistical analysis and reporting. *J Natl Cancer Inst*. 2007;99:147-57.
8. Abbod MF, Catto JW, Linkens DA, Hamdy FC. Application of artificial intelligence to the management of urological cancer. *J Urol*. 2007;178:1150-6.
9. Khan J, Wei JS, Ringner M, Saal LH, Ladanyi M, Westermann F, et al. Classification and diagnostic prediction of cancers using gene expression profiling and artificial neural networks. *Nat Med*. 2001;7:673-9.
10. Lancashire LJ, Powe DG, Reis-Filho JS, Rakha E, Lemetre C, Weigelt B, et al. A validated gene expression profile for detecting clinical outcome in breast cancer using artificial neural networks. *Breast Cancer Res Treat*. 2009.
11. Brown MP, Grundy WN, Lin D, Cristianini N, Sugnet CW, Furey TS, et al. Knowledge-based analysis of microarray gene expression data by using support vector machines. *Proc Natl Acad Sci U S A*. 2000;97:262-7.
12. Huang TM, Kecman V. Gene extraction for cancer diagnosis by support vector machines--an improvement. *Artif Intell Med*. 2005;35:185-94.

13. Schwarzer G, Vach W, Schumacher M. On the misuses of artificial neural networks for prognostic and diagnostic classification in oncology. *Stat Med.* 2000.
14. Hastie T, Tibshirani R, Friedman J. *The Elements of Statistical Learning: Data Mining, Inference and Prediction.* New York: Springer-Verlag; 2001.
15. Catto JW, Abbod MF, Linkens DA, Hamdy FC. Neuro-fuzzy modeling: an accurate and interpretable method for predicting bladder cancer progression. *J Urol.* 2006;175:474-9.
16. Catto JW, Abbod MF, Linkens DA, Larre S, Rosario DJ, Hamdy FC. Neurofuzzy modeling to determine recurrence risk following radical cystectomy for non-metastatic urothelial carcinoma of the bladder. *Clin Cancer Res.* 2009; 15(9):3150-5.
17. Wild PJ, Herr A, Wissmann C, Stoehr R, Rosenthal A, Zaak D, et al. Gene expression profiling of progressive papillary noninvasive carcinomas of the urinary bladder. *Clin Cancer Res.* 2005;11:4415-29.
18. van Oers JM, Wild PJ, Burger M, Denzinger S, Stoehr R, Roskopf E, et al. FGFR3 mutations and a normal CK20 staining pattern define low-grade noninvasive urothelial bladder tumours. *Eur Urol.* 2007;52:760-8.
19. Chen M, Linkens DA. A systematic neurofuzzy modelling framework with application to material property prediction. *IEEE Trans SMC Part B: Cybernetics.* 2001;31(5):781-90.
20. Abbod MF, Catto JWF, Chen M, Linkens DA, Hamdy FC. Artificial intelligence for the prediction of bladder cancer. *Biomed Eng Appl Basis Comm.* 2004;16:49-58.
21. Molinaro AM, Simon R, Pfeiffer RM. Prediction error estimation: a comparison of resampling methods. *Bioinformatics.* 2005;21:3301-7.
22. Catto JWF, Xinarianos G, Burton JL, Meuth M, Hamdy FC. Differential expression of hMLH1 and hMSH2 is related to bladder cancer grade, stage and prognosis, but not microsatellite instability. *Int J Cancer.* 2003;105:484-90.
23. Begg CB, Cramer LD, Venkatraman ES, Rosai J. Comparing tumour staging and grading systems: a case study and a review of the issues, using thymoma as a model. *Stat Med.* 2000;19:1997-2014.
24. Catto JWF, Linkens DA, Abbod MF, Chen M, Burton JL, Feeley KM, et al. Artificial Intelligence in Predicting Bladder Cancer Outcome: A Comparison of Neuro-Fuzzy Modeling and Artificial Neural Networks. *Clin Cancer Res.* 2003;9:4172-7.

25. Reedy EA, Heatfield BM, Trump BF, Resau JH. Correlation of cytokeratin patterns with histopathology during neoplastic progression in the rat urinary bladder. *Pathobiology*. 1990;58:15-27.
26. Yamana K, Bilim V, Hara N, Kasahara T, Itoi T, Maruyama R, et al. Prognostic impact of FAS/CD95/APO-1 in urothelial cancers: decreased expression of Fas is associated with disease progression. *Br J Cancer*. 2005;93:544-51.
27. Rieger-Christ KM, Ng L, Hanley RS, Durrani O, Ma H, Yee AS, et al. Restoration of plakoglobin expression in bladder carcinoma cell lines suppresses cell migration and tumorigenic potential. *Br J Cancer*. 2005;92:2153-9.
28. Friedrich MG, Chandrasoma S, Siegmund KD, Weisenberger DJ, Cheng JC, Toma MI, et al. Prognostic relevance of methylation markers in patients with non-muscle invasive bladder carcinoma. *Eur J Cancer*. 2005;41:2769-78.
29. Bektic J, Pfeil K, Berger AP, Ramoner R, Pelzer A, Schafer G, et al. Small G-protein RhoE is underexpressed in prostate cancer and induces cell cycle arrest and apoptosis. *Prostate*. 2005;64:332-40.
30. Bogliolo M, Taylor RM, Caldecott KW, Frosina G. Reduced ligation during DNA base excision repair supported by BRCA2 mutant cells. *Oncogene*. 2000;19:5781-7.

Figure Legends

Fig. 1. The Work flow for this report. Pearson coefficient was used to reduce the 2,800 genes to the 200 most associated with progression. These genes were modelled by separate ANNs and NFMs. For each model 200 iterations were run. Each iteration studied a single gene and consisted of training/validation/testing of the model. The model's error was the score that determined the significance of the gene being tested in that iteration. In the *Selectivity* approach, we changed all 200 gene values to their mean and then individually maximized (largest value seen) and minimized single genes. Following model testing the analysed gene was returned to average before starting the next iteration. This approach hoped to find genes whose extreme presence caused most disruption to the model. In the *Averaging* approach, all 200 genes were left unchanged whilst single individual genes were averaged for their model iteration. This model aimed to find those genes whose loss of profile resulted in most disruption to the model. Gene rankings from these models were then averaged to generate the Committee of models ranking. The highest ranking members were then compared with the Original panel identified by Wild et al [17] by predicting progression in the same UCC cohort. Six members had commercial antibodies and their expression was tested in a new cohort of UCC.

Fig. 2. Performance of the AI models during dimension reduction. (a). The model error for 1-200 genes is shown (RMS value). In general, NFM has a lower error than ANN. A panel with 11 genes has a similar error to that with 158 genes (NFM) or 140 genes

(ANN). (b) Correct progression classifications (percentage) with NFM or ANN using models with n^{1-200} genes.

Fig. 3. The *Committee* panel for Superficial UCC progression prediction. (a). Tumour progression stratified by pathological grade, the *Original* and *Committee* panels. (b). NFM rule base for the *Committee* panel. Probe values are coloured according to value around mean (reduced = red, increased = blue and mean = black).

Fig. 4. Tumor progression using immunohistochemistry for members of the *Committee* panel. (a) Abnormal expression of panel members in UCC (Insert boxes show expression in normal urothelium: strong membranous TNFRSF6 staining; KRT18 confined to umbrella cells; strong nuclear LIG3 and BRCA2 staining; weak membranous DSG2 staining; very weak ICAM1 staining of urothelium and strong staining within the endothelium of capillaries). (b). Tumor progression stratified by grade and the *Committee* panel in the second superficial UCC population (n=134). A bad signature is defined as $\geq 50\%$ proteins with abnormal expression.

Table 1. The two UCC cohorts studied in this report

		i. Gene array tumors		ii. TMA tumors	
		n	%	n	%
Gender	Male	29	85.3%	194	73.8%
	Female	5	14.7%	68	25.9%
Stage TNM 1998	Normal	8	100.0%		
	pTis	3	4.5%		
	pTa	46	69.7%	149	56.7%
	pT1	10	15.2%	49	18.6%
	pT2	7	10.6%	59	22.4%
	pT3			2	0.8%
	pT4			3	1.1%
	PUNLMP	1	1.5%	22	8.4%
Stage TNM 2004	pTis	3	4.5%		
	pTa	45	68.2%	127	48.3%
	pT1	10	15.2%	49	18.6%
	pT2	7	10.6%	59	22.4%
	pT3			2	0.8%
	pT4			3	1.1%
	Grade	Grade 1	27	40.9%	83
	Grade 2	24	36.4%	69	26.2%
	Grade 3	15	22.7%	110	41.8%
Growth pattern	Papillary	55	83.3%	210	79.8%
	Solid	11	16.7%	51	19.4%
	Unknown			1	0.4%
Multiplicity	Unifocal	29	43.9%	54	20.5%
	Multifocal	37	56.1%	208	79.1%
Carcinoma in situ	No pTis	62	93.9%	227	86.3%
	pTis	4	6.1%	35	13.3%
Tumor	Metastasis			2	0.8%
	Primary UCC	25	37.9%	255	97.0%
	Recurrent UCC	41	62.1%	5	1.9%
	Progression rate	10/34*	29.4%	36/134***	26.9%
Median (range) time to progression		21 (0-60) months		23 (1-154) months	
Overall survival		unknown		167/198	84.3%
Median (range) overall survival time**		43 (0-109) months		90 (24-154) months	
Total UCC		66	100.0%	262	100.0%

* in the 34 individual patients

** in non-progressing patients

*** in 134 primary superficial tumors with available follow up information

Table 2. The *Committee* gene panel selected according to ranking frequency from AI models

	Symbol	Gene name	Function
1	<i>PP</i>	Pyrophosphatase (inorganic)	Phosphate metabolism / metabolism
2	<i>TNFRSF6</i>	TNF receptor family member 6 (CD95)	Apoptosis / immune response / signal transduction
3	<i>LIG3</i>	DNA Ligase III	Cytokinesis / DNA replication & repair / meiosis
4	<i>BRCA2</i>	Breast cancer type 2 susceptibility gene	Cell cycle control / double-strand break repair / DNA replication / chromatin architecture / apoptosis
5	<i>ICAM1</i>	Intercellular adhesion molecule 1 (CD54)	Cell-cell adhesion
6	<i>ARHE</i>	Ras homolog gene family, member E	Cell adhesion / signal transduction / cytoskeleton organization
7	<i>NACA</i>	nascent-polypeptide-associated complex α	Protein biosynthesis / nascent polypeptide association
8	<i>DSG2</i>	Desmoglein 2	Cell adhesion / homophilic cell adhesion
9	<i>KRT18</i>	Keratin 18	Embryogenesis and morphogenesis
10	<i>FLJ14146</i>	Uncharacterized protein C1orf115	Unknown function
11	<i>TP53BP2</i>	p53 binding protein 2 (ASPP2)	Cell cycle/ apoptosis regulation / signal transduction

Genes shown in bold were analysed by immunohistochemistry

Table 3. Immunohistochemical analysis of 263 bladder tumors for *LIG3*, *BRCA2*, *TNFRSF6*, *KRT18*, *DSG2* and *ICAM1*

	<i>TNFRSF6</i>		<i>LIG3</i>		<i>ICAM1</i>		<i>DSG2</i>		<i>BRCA2</i>		<i>KRT18</i>	
	Abnormal / Total	χ^2	Abnormal / Total	χ^2	Abnormal / Total	χ^2	Abnormal / Total	χ^2	Abnormal / Total	χ^2	Abnormal / Total	χ^2
Grade												
1	16/69	28%	42/66	64%	46/61	75%	35/67	52%	23/69	33%	29/61	48%
2	15/65	23%	44/66	67%	41/62	66%	37/65	57%	22/66	33%	30/60	50%
3	13/93	14%	33/95	35%	40/93	43%	63/93	68%	40/95	42%	46/88	52%
		0.093		0.0001		0.0001		0.119		0.398		0.850
Stage												
PUNLMP	7/19	37%	10/18	56%	11/16	69%	12/18	67%	5/18	28%	7/16	44%
pTa	28/112	25%	70/110	64%	72/103	70%	55/109	51%	37/113	33%	51/100	51%
pT1	6/42	14%	17/43	40%	26/44	59%	31/43	72%	18/42	43%	21/41	51%
pT2	6/49	12%	21/51	41%	18/48	38%	34/50	68%	23/52		24/48	50%
pT3	0/2	0%	0/2	0%	0/2	0%	1/2	50%	0/2	0%	2/2	100%
pT4	0/3	0%	1/3	33%	0/3	0%	2/3	66%	2/3	67%	0/2	0%
		0.119		0.018		0.001		0.128		0.344		0.506
CIS												
Absent	42/200	21%	110/198	69%	115/189	61%	117/169	60%	75/201	37%	90/182	50%
Present	5/27	19%	9/29	31%	12/27	44%	18/29	62%	10/29	35%	15/27	56%
		0.765		0.014		0.105		0.807		0.768		0.554
Growth												
Papillary	42/187	23%	99/185	53%	115/177	63%	103/184	56%	69/187	37%	88/170	52%
Solid	4/39	10%	20/41	49%	14/38	37%	31/40	78%	15/42	36%	17/38	45%
		0.085		0.583		0.003		0.012		0.886		0.433
Progression free survival*												
Progression	12/34	35%	21/33	64%	17/31	55%	23/33	70%	13/33	40%	17/30	57%
No	10/84	12%	48/83	58%	54/78	69%	42/81	52%	31/84	37%	35/72	49%
		0.003		0.566		0.155		0.081		0.802		0.458

* Only superficial tumors were analyzed for this outcome

NOTE. For each variable the numerator is the number of abnormally immunostained tumours and the denominator is the number successfully analyzed for that protein

Figure 1
[Click here to download high resolution image](#)

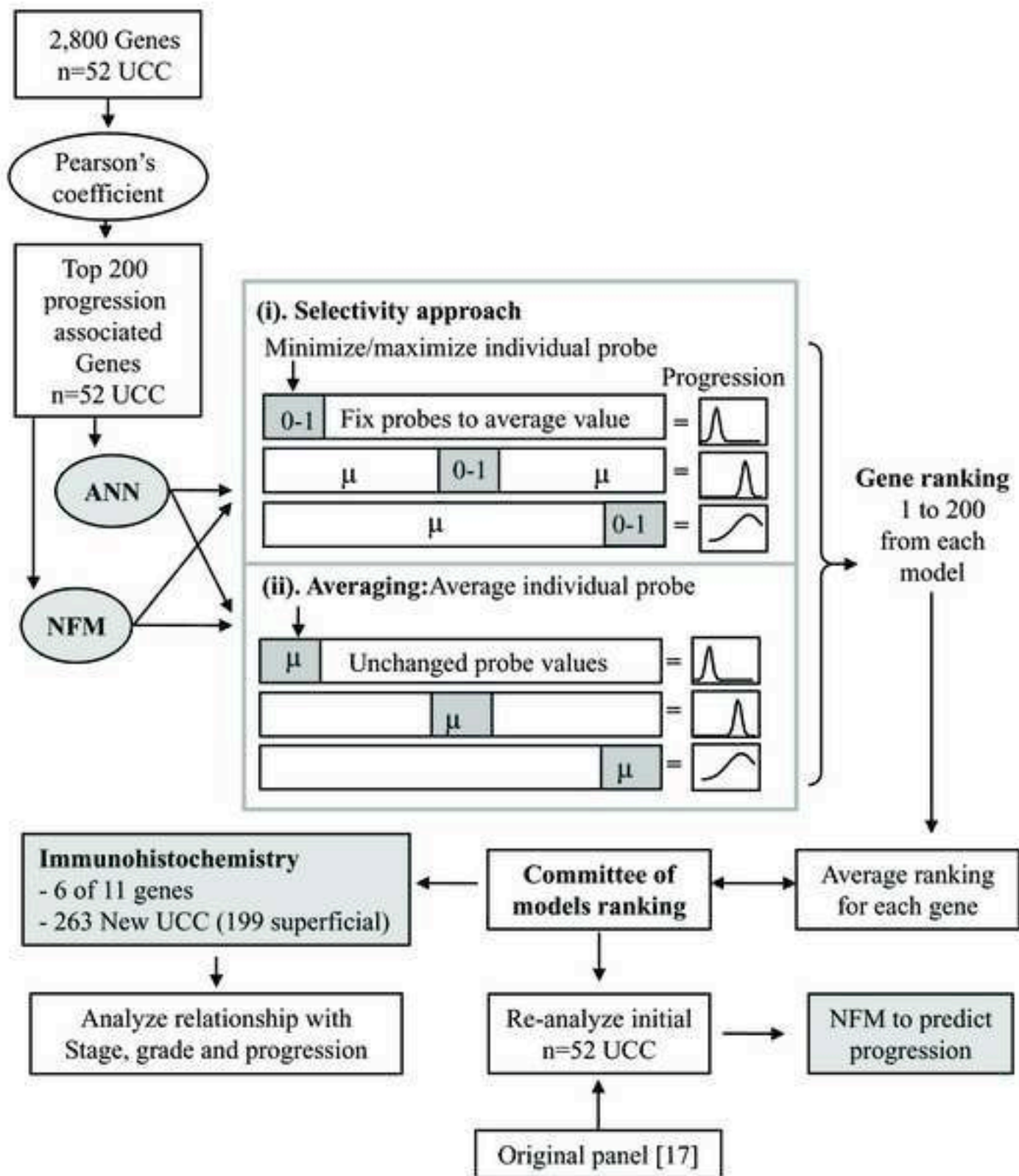


Figure 1. Work flow for this report.

Figure 2
[Click here to download high resolution image](#)

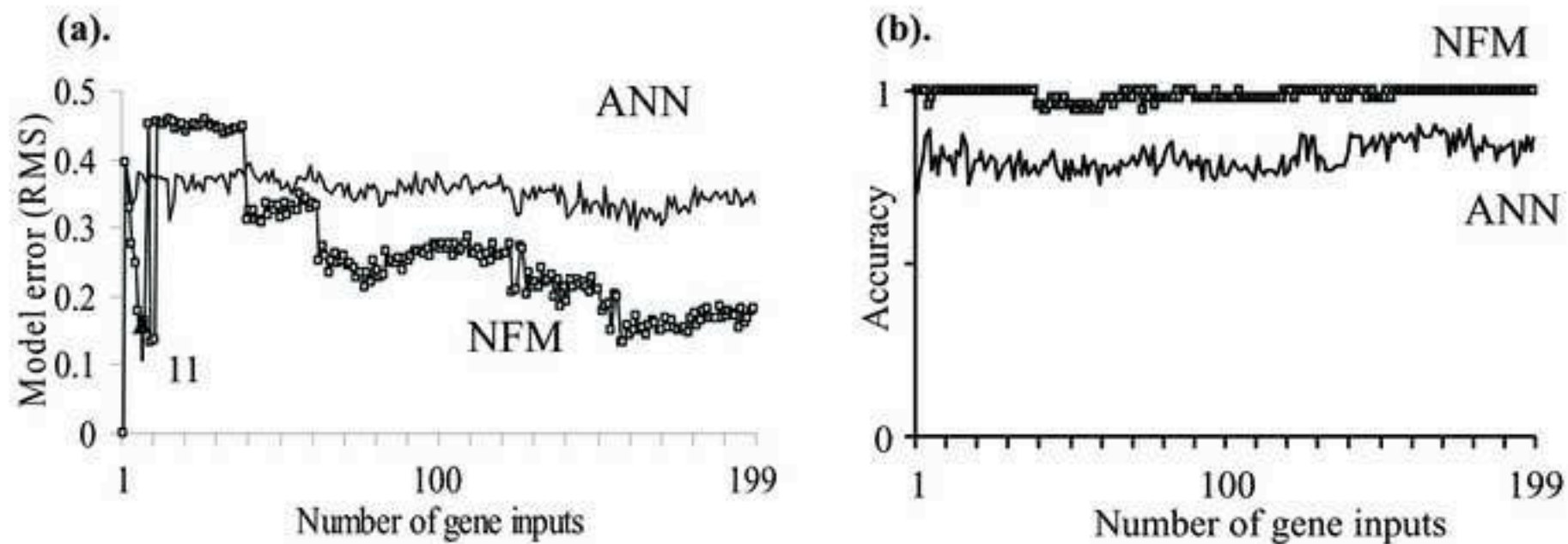


Figure 2. Performance of the AI models during dimension reduction.

Figure 3
[Click here to download high resolution image](#)

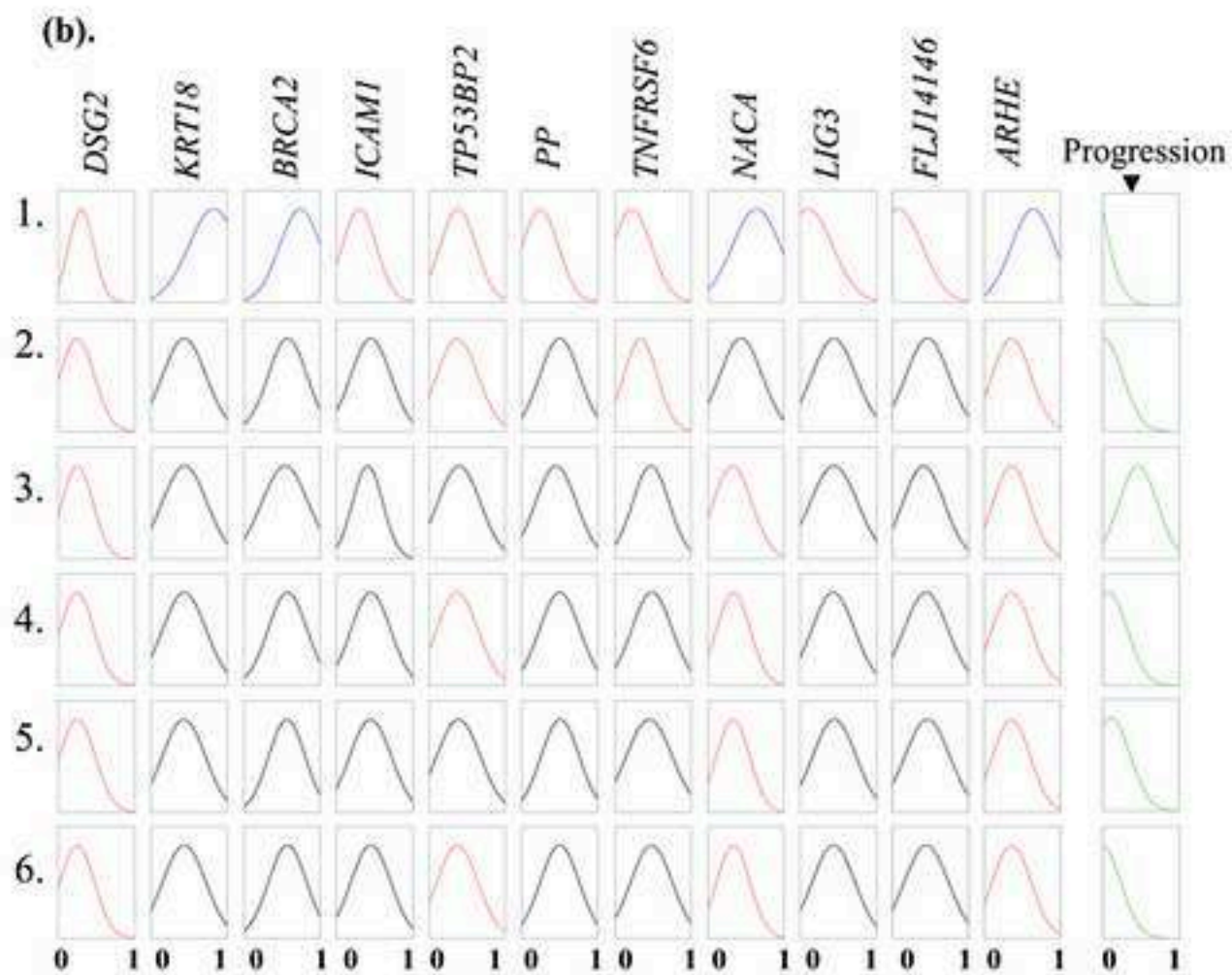
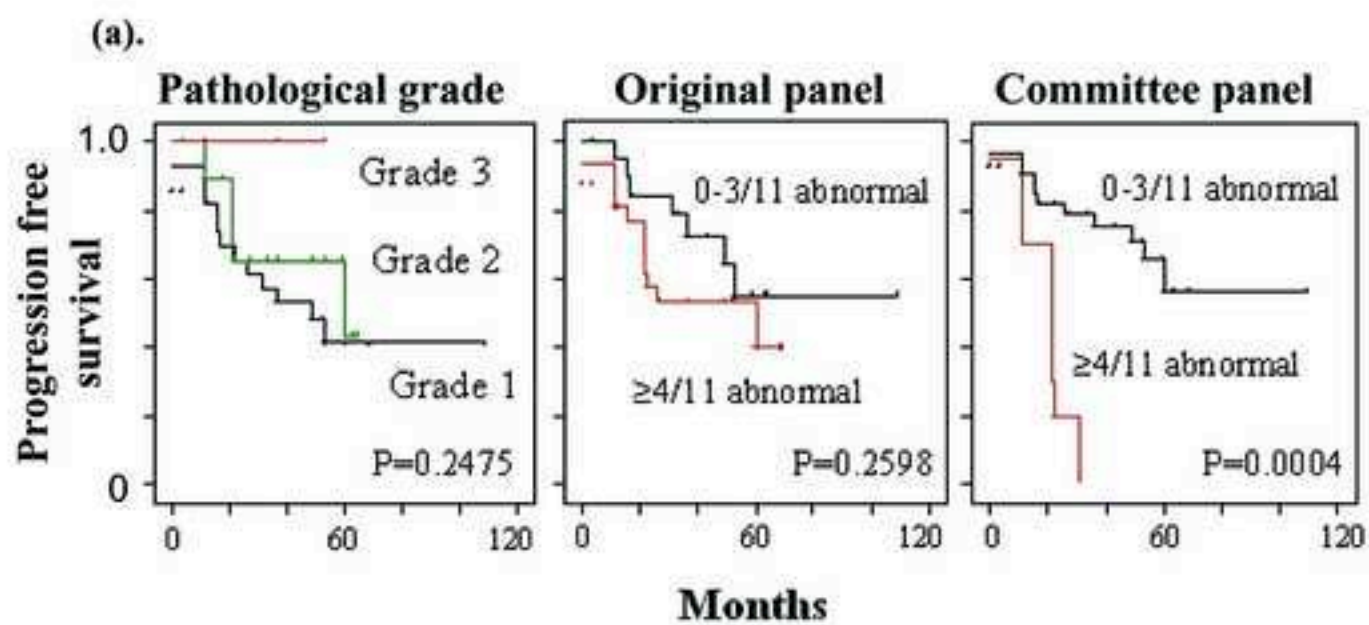
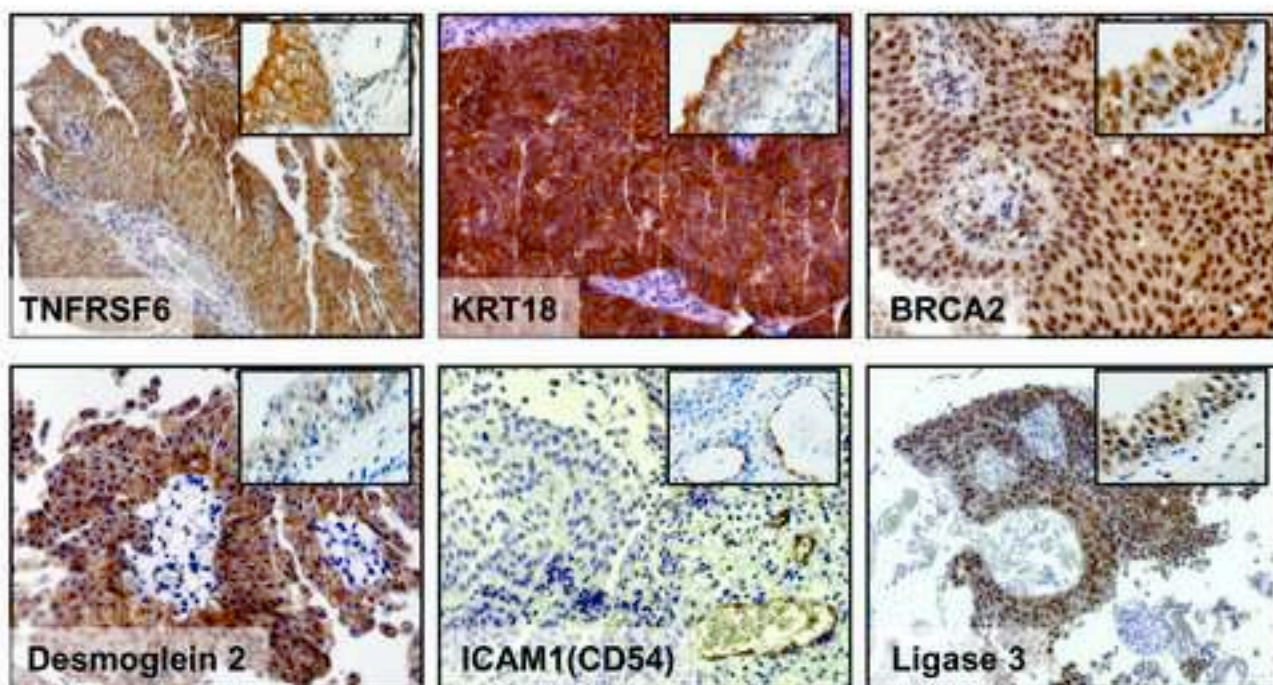


Figure 3. The Committee panel for Superficial UCC progression prediction.

(a).



(b).

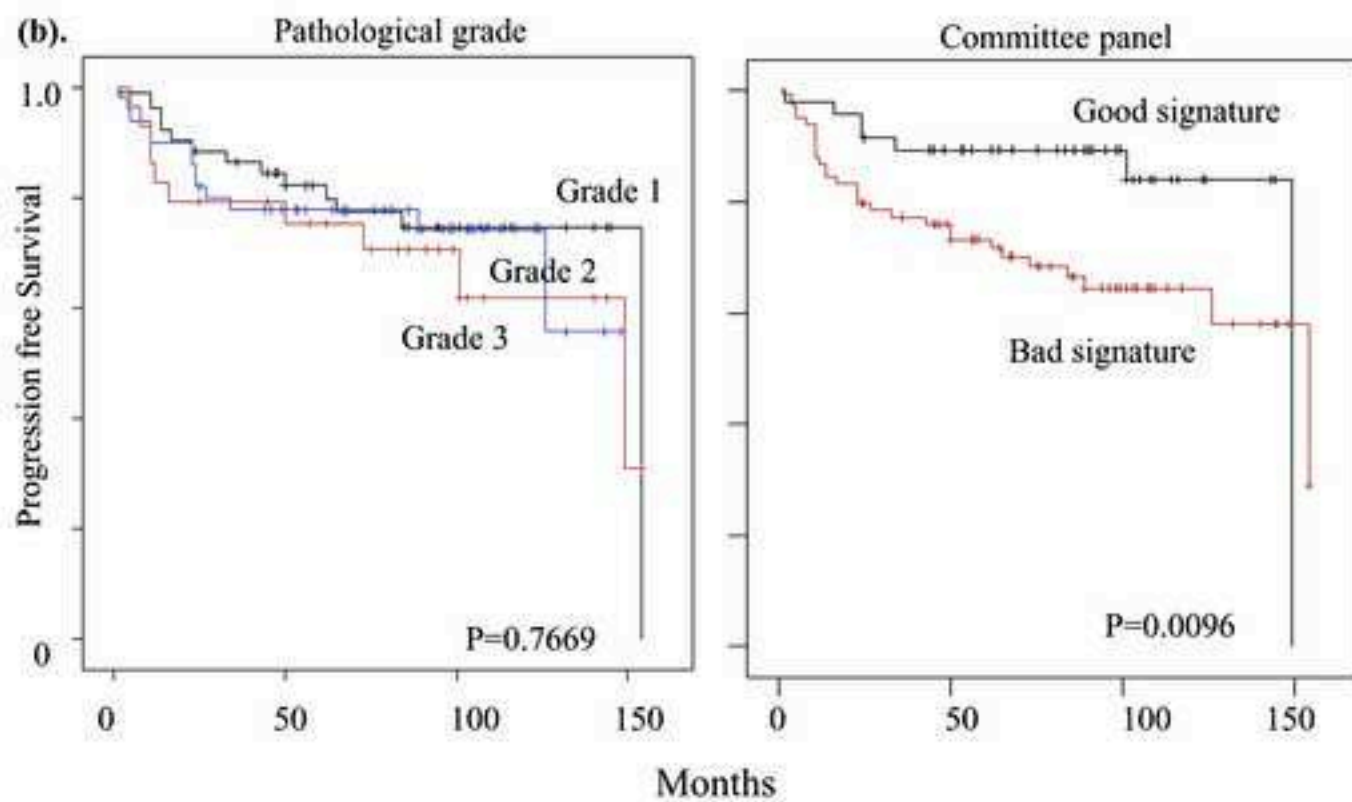


Figure 4. Tumor progression using immunohistochemistry for members of the Committee panel.